International Forum on Aeroelasticity and Structural Dynamics
IFASD 2019
9-13 June 2019, Savannah, Georgia, USA

# AIRCRAFT-FUEL SLOSHING ROMS FOR AEROELASTIC ANALYSES

**Franco Mastroddi[1], Francesco Saltari[1], Michael Wright[2], Arnaud G. Malan[2], Simone Simeone[3], Francesco Gambioli[3]**

[1]Dept. of Mechanical and Aerospace Engineering
Sapienza University of Rome
Via Eudossiana 18, 00184 Rome, Italy
franco.mastroddi@uniroma1.it

[2]Industrial CFD Research Group
Department of Mechanical Engineering
University of Cape Town
Rondebosch, Cape Town 7701, South Africa

[3]Loads & Aeroelastics Dept.
Airbus Operation Ltd
Filton, Bristol BS34 7PA, United Kingdom

**Keywords:** Sloshing, Aeroelasticity, Reduced-Order Modeling

**Abstract:** This paper will propose Reduced-Order Models (ROM) based on data provided by high-fidelity and highly efficient CFD codes, for the study of sloshing-integrated aeroelastic systems. A sloshing-addressed CFD code, ELEMENTAL®, is employed to generate data set to be used for the ROM synthesis. The developed sloshing ROM, based on a Linearized Frequency Domain (LFD) approach, uses an Input/Output system identification technique from CFD transient simulations to construct an unsteady Generalized Sloshing Force (GSF) matrix in analogy with the Generalized Aerodynamic Force (GAF) matrix used to model the aircraft external unsteady aerodynamics. The approach is assessed with experimental results performed at the Airbus Protospace Lab. (Filton, Bristol UK) on an actual beam-like structure carrying a series of tanks. The obtained state-space form for the sloshing ROM has been suitable developed for applying it within aeroelastic framework for perspective integrated stability analyses and design.

## 1 INTRODUCTION

The effects of wing tank-fuel sloshing are not typically included in the aeroelastic analysis and design although these effects might be significant to be taken into account in the design process. Indeed, the tank-fuel sloshing is typically simply modeled by including *a posteriori* a suitable damping coefficient in the final aeroelastic aircraft model.
Many literature contributions are present in the field of CFD simulations for reaching, on one side, an adequate level of fidelity on sloshing phenomenon and, on the other side, an acceptable level of computational effort for using these models at design level. A key example relevant to aircraft fuel slosh is the development of a fast and efficient framework [3]. This work was followed by application to a wide range of aircraft operational conditions [2].

The trade-off between model accuracy and computational effort characterized the development of unsteady-aerodynamic modeling in the past three decades so stimulating the use of ROM's which allowed to exploit high fidelity aerodynamic description for aeroelastic analysis and design, Ref. [1]. Specifically, the capability to find via ROM procedure a linearized aerodynamic operator became so mature to be applied not only for aircraft aeroelastic analysis and design (Ref. [6]), but also in other aerospace applications as launch vehicle aeroelasticity in atmospheric flight (Refs. [4, 5]).
In the present paper a linearizing ROM procedure – namely, a Linear Frequency Domain approach, LFD – for describing the sloshing pressure distribution ($p_S$) as given by a tank-wall motion is proposed in analogy to that typically performed for the external aerodynamic pressure distribution $p_A$, (see Fig. 1). In Section 2 the sloshing-addressed CFD code, ELEMENTAL®,

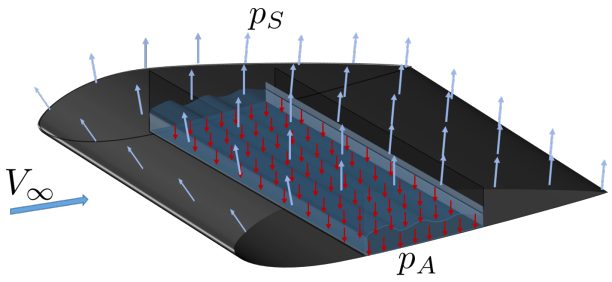


Figure 1: Wing external pressure distribution as given by the aerodynamic pressure $p_A$ (blue arrows) and and tank internal pressure distribution $p_S$ (red arrows) as given by sloshing fuel.

that will be used as data-set generator for the ROM synthesis, is introduced. In Section 3 the ROM model for the sloshing-fuel system, based on a LFD approach, is introduced and the coupled model of this system with the wing aeroelastic system is addressed as well. Next, in Sections 4 the obtained results are presented and also compared with the experimental results performed at the Airbus Protospace Lab. (Filton, Bristol UK) on an actual beam-like structure carrying a series of tanks. Finally, in Section 5 some concluding remarks are presented.

## 2 A SLOSHING ADDRESSED CFD DESCRIPTION: ELEMENTAL®

CFD high-fidelity/high-efficiency analyses were performed by using ELEMENTAL®. ELEMENTAL is a volume-of-fluid (VOF) code and has been extensively tested and proven accurate as compared to even violent slosh found in aircraft [3], [2], and [7]. The cited work critically assesses accuracy via comparison of CFD predicted tank pressure to experimental data. Average accuracies for high fill level cases are to -with-in $10\%$ to $15\%$ in terms of slosh induced tank wall pressures.

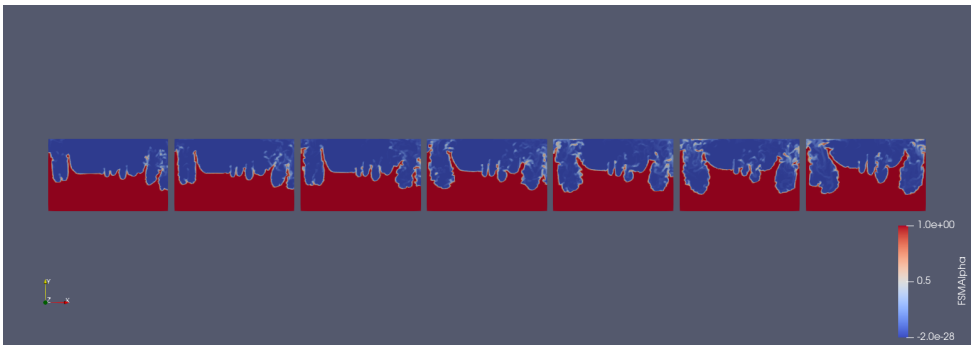


Figure 2: ELEMENTAL prediction of free surface evolution at $t = 0.2s$.

A 2D CFD model of the above mentioned recent Airbus experiment has been developed. To date, this has been via applying the measured acceleration to the tank. The resulting simulated free-surface-evolution is shown in Fig. 2.

## 3 A CFD-BASED ROM MODEL FOR SLOSHING FUEL SYSTEM AND ITS FULLY COUPLED INTEGRATION WITH THE AEROELASTIC SYSTEM.

In the present Section the obtained ROM model for sloshing will be derived. The structural displacements $\mathbf{u}(\mathbf{x}, t)$ can be expressed by the spectral decomposition

$$\mathbf{u}(\mathbf{x}, t) \simeq \sum_{n=1}^{N} \boldsymbol{\psi}_n(\mathbf{x}) q_n(t) \tag{1}$$

where $\boldsymbol{\psi}_n(\mathbf{x})$ are the modes of vibrations of the structure and $q_n(t)$ are the generalized coordinates describing the body deformation in time. Note that a space-discretization for the structure is assumed by including a finite number $N$ of modes in the analysis, *i.e.,* a frequency-band-limited unsteady process. Considering this displacement representation for aircraft wing dynamics, one has the following Lagrange equations of motion in terms of N modal coordinates $q_n(t)$

$$\mathsf{M}\ddot{\mathsf{q}} + \mathsf{K}\mathsf{q} = \mathsf{e} + \mathsf{g} + \mathsf{f}^{(ext)} \tag{2}$$

where $\mathsf{q} = [q_1, q_2, \ldots, q_N]^{\mathrm{T}}$ is the modal coordinates vector, $\mathsf{M}$ and $\mathsf{K}$ are, respectively, the modal mass and stiffness (diagonal) matrices, whereas $\mathsf{e} = [e_1, e_2, \ldots, e_N]^{\mathrm{T}}$ and $\mathsf{g} = [g_1, g_2, \ldots, g_N]^{\mathrm{T}}$ are, respectively, the generalized *aerodynamic* and *sloshing* forces induced by the elastic motion and evaluated via linearization ROM process by using 3D CFD unsteady simulations. The $\mathsf{f}^{(ext)}$ is the vector of the current external forcing terms. Note that the *generalized-sloshing-force* vector is obtained by projecting the pressure distribution $p_S$ on each n-th modal shape $\boldsymbol{\psi}_n$ by integrating the inner product on the tank wet surface $\mathcal{S}_{tank}$ as in the following ($\mathbf{n}$ unit normal vector to $\mathcal{S}_{tank}$)

$$g_n = -\oiint_{\mathcal{S}_{tank}} p_S \; \mathbf{n} \cdot \boldsymbol{\psi}_n \, d\mathcal{S} \tag{3}$$

In accordance with the similar procedure used for unsteady aerodynamics, a linearized description for the sloshing forces acting on the tank walls is here proposed (see Ref. [6]).

### 3.1 Evaluation of GSF matrix via Linearized Frequency Domain (LFD) approach

The linearized description of the unsteady sloshing forces linearly dependent on the modal coordinates by means of a matrix operator $\mathsf{G}$ (*Generalized Sloshing Force*, GSF, matrix) is introduced in Laplace domain as

$$\tilde{g}_n \;\; = \;\; \sum_{m=1}^{N} G_{nm}(s) \tilde{q}_m \tag{4}$$

The key point is how to determine the transfer function matrix for the unsteady sloshing operator $\mathsf{G}$ by using an Input/Output system identification technique from a number of CFD transient simulations. The basic assumption is that only a limited number of inputs mode shapes, and a correspondingly small number of outputs, that is, generalized forces, are enough to describe the physics of the problem within a limited frequency band of interest. Indeed, one may construct the *GSF* matrix first by considering its definition in Fourier angular frequency sub-domain $\omega$

by the position $s = j\omega$. Thus, a time-domain variation of the boundary conditions as input for sloshing dynamics is imposed in the CFD code by moving the tank boundaries following the space description of each structural mode shape. The time input function used for animating the $m$-th mode shape is generally a small amplitude Gaussian-like function (Refs. [4–6]) as $q_m(t) = A_m \exp\left[-\left(\frac{(t-T/2)}{\kappa T}\right)^2\right]$ By evaluating via ELEMENTAL® the corresponding sloshing pressure field $p_S^{(m)}$ and then projecting it (see Eq. 3) on the generic $n$-th mode shape, one obtain the time domain generalized quantities $g_n^{(m)}(t)$. Once these quantities are Fourier transformed into $\tilde{g}_n^{(m)}(\omega)$, one can finally obtain the following LFD estimate of the GSF matrix as

$$G_{nm}(\omega) = \tilde{g}_n^{(m)}(\omega) \,/\, \tilde{q}_m(\omega) \tag{5}$$

The extension of this matrix frequency dependent to the Laplace domain represents the introduced transfer function sloshing operator.
Thus, the equation of the sloshing-integrated *structural* response in Laplace domain is given by

$$\left[s^2\mathsf{M} + \mathsf{K} - \mathsf{G}(s)\right]\tilde{\mathsf{q}} - \mathsf{M}\left(s\mathsf{q}_0 + \dot{\mathsf{q}}_0\right) \,=\, 0 \tag{6}$$

where $\mathsf{q}_0$ and $\dot{\mathsf{q}}_0$ are the modal displacement and velocity vector respectively at the initial time. The above model could be used to obtain the vector $\tilde{\mathsf{q}}$ as given by assigned initial conditions as in the performed experiment so allowing a direct comparison with the experimental results.

### 3.2 State-Space forms of GSF matrix inspired by Equivalent Mechanical Models

In order to have a component description of the coupled sloshing/structure/aerodynamic system, frequency-interpolated forms for the GSF matrix evaluated by CFD data (given by LFD linearization via Eq. 5) are introduced in a very similar way as the so-called finite-state aerodynamic is introduced in aeroelasticity for modelling the unsteady aerodynamic forces (Refs. [8], [9], [10]). More specifically, two different interpolation approaches were considered depending on the level of nonlinearity of the sloshing phenomenon under investigation.

In the first case of *lateral* sloshing, namely, a sloshing phenomenon almost linearly dependent on input tank motion, the reference to the equivalent Mechanical Model (EMM) (Refs. [11], [12]) suggested as interpolating structure in frequency domain the following relationship:

$$\begin{aligned}\begin{Bmatrix}\tilde{f}_y^{t_i}\\ \tilde{M}^{t_i}\end{Bmatrix} &= \left[(j\omega)^2\hat{\mathsf{A}}^{t_i} + \left[(j\omega)^2\hat{\mathsf{B}}^{t_i} + \hat{\mathsf{C}}^{t_i}\right]\left[(j\omega)^2\mathsf{I}^{t_i} + (j\omega)\hat{\mathsf{D}}^{t_i} + \hat{\Omega}^{2^{t_i}}\right]^{-1}\left[(j\omega)^2\hat{\mathsf{B}}^{t_i} + \hat{\mathsf{C}}^{t_i}\right]^{\mathrm{T}}\right]\begin{Bmatrix}\tilde{y}^{t_i}\\ \tilde{\varphi}^{t_i}\end{Bmatrix}\\ &= \hat{\mathsf{G}}_{int}^{t_i}(\omega)\begin{Bmatrix}\tilde{y}^{t_i}\\ \tilde{\varphi}^{t_i}\end{Bmatrix}\end{aligned} \tag{7}$$

where $\tilde{y}^{t_i}$ and $\tilde{\varphi}^{t_i}$ are the Fourier transforms of rigid body lateral translation and rotation of the $i-th$ tank (with rotation vector orthogonal to lateral-translation direction and to the gravity direction), and $\tilde{f}_y^{t_i}$ and $\tilde{M}^{t_i}$ the Fourier transforms of the corresponding lateral force and moment applied by the sloshing fluid to the tank. Moreover, $\hat{\mathsf{A}}^{t_i}$ is a $2 \times 2$ simmetric matrix, $\hat{\mathsf{B}}^{t_i}$ and $\hat{\mathsf{C}}^{t_i}$ are $2 \times N_{sm}$ matrices, and $\mathsf{I}^{t_i}$, $\hat{\mathsf{D}}^{t_i}$ and $\hat{\Omega}^{2^{t_i}}$ are diagonal $N_{sm} \times N_{sm}$ matrices. Note that the previous matrices are to be determined in order to fit the values of the GSF matrix as it will be later clarified.

In the second case of *vertical* sloshing, namely, a phenomenon that triggers only in presence of Rayleigh-Taylor instability with relevant damping effects due to the dissipation of energy

caused by the free surface breakage, the following interpolating function in frequency domain is proposed in order to fit the frequency domain data evaluated by Eq. 5:

$$\begin{aligned}\tilde{f}_z^{t_i} &= \left[(j\omega)^2 \check{A}^{t_i} + \check{\mathsf{B}}^{t_i}\left[(j\omega)^2 \mathsf{I}^{t_i} + (j\omega)\check{\mathsf{D}}^{t_i} + \check{\Omega}^{2^{t_i}}\right]^{-1} \tilde{\mathsf{C}}^{t_i}(j\omega)^2\right] \tilde{z}^{t_i} \\ &= \check{G}_{int}^{t_i}(\omega)\, \tilde{z}^{t_i} \end{aligned} \tag{8}$$

where $\tilde{z}^{t_i}$ is now the Fourier transform of rigid body vertical translation of the $i-th$ tank, and $\tilde{f}_z^{t_i}$ the Fourier transforms of the corresponding vertical force and applied by the sloshing fluid to the tank. Moreover, $\check{A}^{t_i}$ is now assumed as $1 \times 1$ coefficient, $\check{\mathsf{B}}^{t_i}$ and $\check{\mathsf{C}}^{t_i}$ are, respectively, $1 \times N_{sm}$ and $N_{sm} \times 1$ matrices ($N_{sm}$ number of assumed sloshing modes), and $\mathsf{I}^{t_i}$, $\check{\mathsf{D}}^{t_i}$ and $\check{\Omega}^{2^{t_i}}$ are diagonal $N_{sm} \times N_{sm}$ matrices. Also these matrices are to be determined in order to fit the values of the GSF matrix as it will be later clarified.

Note that for both the proposed interpolating structure, the matrices $\hat{\Omega}^{2^{t_i}}$, $\check{\Omega}^{2^{t_i}}$, $\hat{\mathsf{D}}^{t_i}$, and $\check{\mathsf{D}}^{t_i}$ are currently representing the (square of the) natural frequency and damping modal coefficients of the sloshing modes for the $i-th$ tanks.

Next, transformation matrices like $\hat{\mathsf{T}}^{t_i}$ and $\check{\mathsf{T}}^{t_i}$ are introduced for each generic $i-th$ tank for obtaining the tank state space variables $\left\{\tilde{y}^{t_i}, \tilde{\varphi}^{t_i}\right\}^{\mathrm{T}}$ and $\tilde{z}^{t_i}$ by the structural modal coordinate vector $\mathsf{q}$ of the hosting structure and tanks (included) as

$$\begin{Bmatrix} \tilde{y}^{t_i} \\ \tilde{\varphi}^{t_i} \end{Bmatrix} = \hat{\mathsf{T}}^{t_i}\, \tilde{\mathsf{q}} \qquad \tilde{z}^{t_i} = \check{\mathsf{T}}^{t_i}\, \mathsf{q} \tag{9}$$

where each columns of the transformation matrices contain, for each corresponding natural modes of vibration of the structure, the components of the modes in terms of translation and rotation for all the considered tanks. Similar relationships can be introduced for evaluating, for each tank, the contribution on the modal forces given by the lateral and vertical sloshing force, or

$$\tilde{\hat{\mathsf{g}}}^{t_i} = \hat{\mathsf{T}}^{t_i{}^{\mathrm{T}}} \begin{Bmatrix} \tilde{f}_y^{t_i} \\ \tilde{M}^{t_i} \end{Bmatrix} \qquad \tilde{\check{\mathsf{g}}}^{t_i} = \check{\mathsf{T}}^{t_i{}^{\mathrm{T}}}\, \tilde{f}_z^{t_i} \tag{10}$$

Thus, considering all the sloshing contribution of all the tank for all lateral and vertical sloshing typology, Eqs. 7, 8, 9, and 10, one has for the total generalized sloshing force vector

$$\tilde{\mathsf{g}} = \sum_{i=1}^{N_{tank}} \left(\tilde{\hat{\mathsf{g}}}^{t_i} + \tilde{\check{\mathsf{g}}}^{t_i}\right) = \sum_{i=1}^{N_{tank}} \left(\hat{\mathsf{T}}^{t_i{}^{\mathrm{T}}} \hat{\mathsf{G}}_{int}^{t_i}(\omega) \hat{\mathsf{T}}^{t_i} + \check{\mathsf{T}}^{t_i{}^{\mathrm{T}}} \check{G}_{int}^{t_i}(\omega) \check{\mathsf{T}}^{t_i}\right) \tilde{\mathsf{q}} = \mathsf{G}_{ROM}(\omega)\tilde{\mathsf{q}} \tag{11}$$

and, therefore, the final ROM GSF matrix $\mathsf{G}_{ROM}(\omega)$ is defined as

$$\mathsf{G}_{ROM}(\omega) = \sum_{i=1}^{N_{tank}} \left(\hat{\mathsf{T}}^{t_i{}^{\mathrm{T}}} \hat{\mathsf{G}}_{int}^{t_i}(\omega) \hat{\mathsf{T}}^{t_i} + \check{\mathsf{T}}^{t_i{}^{\mathrm{T}}} \check{G}_{int}^{t_i}(\omega) \check{\mathsf{T}}^{t_i}\right) \tag{12}$$

The evaluation of the interpolation-coefficient matrices in Eqs. 7 and 8 can be determined by the knowledge of frequency domain data provided after a a single *lateral* or *vertical* CFD simulation for any $i-th$ tank, namely, by the knowledge of the matrices $\hat{\mathsf{G}}_{CFD}^{t_i}(\omega_k)$ and $\check{G}_{CFD}^{t_i}(\omega_k)$ by using a linearization formula identical to 5 but specifically referred to the tank motion (lateral and vertical) and to the forces and moment applied to any tank as single rigid body. Such data are evaluated for a limited set of angular frequencies $\omega_k$ ($k = 1, 2, ..., N_{freq}$).

Finally, the interpolation coefficient matrices $\hat{\mathsf{A}}^{t_i}$, $\hat{\mathsf{B}}^{t_i}$, $\hat{\mathsf{C}}^{t_i}$, $\hat{\mathsf{D}}^{t_i}$, and $\hat{\Omega}^{2^{t_i}}$ for the form adopted in Eq. 7, and the $1 \times 1$ matrices $\check{A}^{t_i}$, $\check{\mathsf{B}}^{t_i}$, $\check{\mathsf{C}}^{t_i}$, $\check{\mathsf{D}}^{t_i}$, and $\check{\Omega}^{2^{t_i}}$ for the form adopted in Eq. 8, are obtained by imposing the following minimum problems

$$\sum_{k=1}^{N_{freq}} \left\| \hat{\mathsf{G}}^{t_i}_{int}(\omega_k) - \hat{\mathsf{G}}^{t_i}_{CFD}(\omega_k) \right\| = \min_{\hat{\mathsf{A}}^{t_i}\hat{\mathsf{B}}^{t_i}\hat{\mathsf{C}}^{t_i}\hat{\mathsf{D}}^{t_i}\hat{\Omega}^{2^{t_i}}} \tag{13}$$

and

$$\sum_{k=1}^{N_{freq}} \left\| \check{G}^{t_i}_{int}(\omega_k) - \check{G}^{t_i}_{CFD}(\omega_k) \right\| = \min_{\check{A}^{t_i}\check{\mathsf{B}}^{t_i}\check{\mathsf{C}}^{t_i}\check{\mathsf{D}}^{t_i}\check{\Omega}^{2^{t_i}}} \tag{14}$$

Namely, the interpolation coefficients are determined minimizing the error, in a assigned frequency band, existing between the CFD evaluated matrices $\hat{\mathsf{G}}^{t_i}_{CFD}(\omega_k)$ and $\check{G}^{t_i}_{CFD}(\omega_k)$, and the interpolating matrices $\hat{\mathsf{G}}^{t_i}_{int}(\omega_k)$ and $\check{G}^{t_i}_{int}(\omega_k)$.

### 3.3 Final hosting-structure/sloshing-fluid reduced model

By introducing the global matrix $\hat{\mathsf{A}}$, $\hat{\mathsf{B}}$, $\hat{\mathsf{C}}$, $\check{\mathsf{A}}$, $\check{\mathsf{B}}$, $\check{\mathsf{C}}$, $\hat{\Omega}^2$, and $\check{\Omega}^2$ as

$$\hat{\mathsf{A}} = \sum_{i=1}^{N_{tank}} \hat{\mathsf{T}}^{t_i\mathrm{T}} \hat{\mathsf{A}}^{t_i} \hat{\mathsf{T}}^{t_i} \qquad \hat{\mathsf{B}} = \sum_{i=1}^{N_{tank}} \hat{\mathsf{T}}^{t_i\mathrm{T}} \hat{\mathsf{B}}^{t_i} \qquad \hat{\mathsf{C}} = \sum_{i=1}^{N_{tank}} \hat{\mathsf{T}}^{t_i\mathrm{T}} \hat{\mathsf{C}}^{t_i}$$

$$\check{\mathsf{A}} = \sum_{i=1}^{N_{tank}} \check{\mathsf{T}}^{t_i\mathrm{T}} \check{A}^{t_i} \check{\mathsf{T}}^{t_i} \qquad \check{\mathsf{B}} = \sum_{i=1}^{N_{tank}} \check{\mathsf{T}}^{t_i\mathrm{T}} \check{\mathsf{B}}^{t_i} \qquad \check{\mathsf{C}} = \sum_{i=1}^{N_{tank}} \check{\mathsf{T}}^{t_i\mathrm{T}} \check{\mathsf{C}}^{t_i}$$

$$\hat{\Omega}^2 = \mathrm{diag}\left\{ \hat{\Omega}^{t_1}, \hat{\Omega}^{t_2}, ..., \hat{\Omega}^{t_{N_{tank}}} \right\}^{\mathrm{T}} \quad \check{\Omega}^2 = \mathrm{diag}\left\{ \check{\Omega}^{t_1}, \check{\Omega}^{t_2}, ..., \check{\Omega}^{t_{N_{tank}}} \right\}^{\mathrm{T}} \tag{15}$$

and by defining the new sloshing global state-space vectors $\tilde{\hat{\mathsf{r}}} = \{\tilde{\hat{\mathsf{r}}}^{t_1}, \tilde{\hat{\mathsf{r}}}^{t_2}, ..., \tilde{\hat{\mathsf{r}}}^{t_{N_{tank}}}\}^{\mathrm{T}}$ and $\tilde{\check{\mathsf{r}}} = \{\tilde{\check{\mathsf{r}}}^{t_1}, \tilde{\check{\mathsf{r}}}^{t_2}, ..., \tilde{\check{\mathsf{r}}}^{t_{N_{tank}}}\}^{\mathrm{T}}$, such that, in Laplace domain

$$\tilde{\hat{\mathsf{r}}}^{t_i} := \left[ s^2 \mathsf{I}^{t_i} + s\hat{\mathsf{D}}^{t_i} + \hat{\Omega}^{2^{t_i}} \right]^{-1} \left[ s^2 \hat{\mathsf{B}}^{t_i} + \hat{\mathsf{C}}^{t_i} \right]^{\mathrm{T}} \hat{\mathsf{T}}^{t_i}\ \tilde{\mathsf{q}} \tag{16}$$

$$\tilde{\check{\mathsf{r}}}^{t_i} := \left[ s^2 \mathsf{I}^{t_i} + s\check{\mathsf{D}}^{t_i} + \check{\Omega}^{2^{t_i}} \right]^{-1} s\check{\mathsf{C}}^{t_i} \check{\mathsf{T}}^{t_i}\ \tilde{\mathsf{q}} \tag{17}$$

one has the final coupled modelling for structure/sloshing in Laplace domain and in a second order form:

$$\left[ \begin{pmatrix} \mathsf{M} - \hat{\mathsf{A}} - \check{\mathsf{A}} & -\hat{\mathsf{B}} & 0 \\ -\hat{\mathsf{B}}^{\mathrm{T}} & \mathsf{I} & 0 \\ 0 & 0 & \mathsf{I} \end{pmatrix} s^2 + \begin{pmatrix} \mathsf{D} & 0 & -\check{\mathsf{B}} \\ 0 & \hat{\mathsf{D}} & 0 \\ -\check{\mathsf{C}} & 0 & \check{\mathsf{D}} \end{pmatrix} s + \begin{pmatrix} \mathsf{K} & \hat{\mathsf{C}} & 0 \\ \hat{\mathsf{C}}^{\mathrm{T}} & \hat{\Omega}^2 & 0 \\ 0 & 0 & \check{\Omega}^2 \end{pmatrix} \right] \begin{Bmatrix} \tilde{\mathsf{q}} \\ \tilde{\hat{\mathsf{r}}} \\ \tilde{\check{\mathsf{r}}} \end{Bmatrix} = 0 \tag{18}$$

where the matrix $\mathsf{D}$ is included to model the damping of the structure with empty tanks.

### 3.4 Final aeroelastic model including sloshing effects

Next, the introduced ROM description for sloshing is extended to aeroelastic system as well. Indeed, the sloshing-integrated *aeroelastic* response in frequency domain is given by (zero time initial conditions):

$$\left[ s^2\mathsf{M} + \mathsf{D} + \mathsf{K} - \mathsf{G}(s) - q_D \mathsf{Q}(s; U_\infty, M_\infty) \right] \tilde{\mathsf{q}} = 0 \tag{19}$$

where the matrix $\mathbf{Q}(s; U_\infty, M_\infty)$ is the so-called it Generalized Aerodynamic Matrix depending on flight conditions (flight speed $U_\infty$ and flight Mach number $M_\infty$) and $q_D$ is the dynamic pressure. Note that the above equation can be used to study the flutter stability of the aircraft including the coupled sloshing effects of fuel by performing a standard eigen aeroelastic analysis searching the poles $s_n$ by imposing the determinant of the above matrix to be zero.

## 4 NUMERICAL RESULTS

In this section some results on sloshing modelling and coupling with the hosting structure are presented in the prespective of using the developed model for wing aeroelastic analysis.

The numerical results are performed on a isolated tank as that used in Ref. [13]. The single tank is parallelepiped, see Fig. 3, with horizontal and vertical dimension equal to $0.1m$ and $0.6m$, whereas the depth is $0.1m$. The considered fill level in all the presented simulation is 50 %.

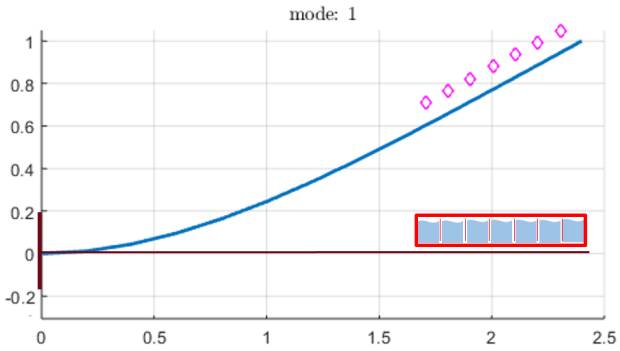


Figure 3: Location of the considered tank cluster on the beam like wing as in the experimental test, Ref. [13] and first vibration mode.

In Figure 4 the trial input time function $q_t(t)$ used as unsteady boundary condition for the CFD code is presented: the analytic function used is the Gaussian $q_t(t) = A_t \exp\left[-\left(\frac{(t-5\sigma_t)}{\sigma_t}\right)^2\right]$ and it is presented in Fig. 4(a) and the related time second derivative in Fig. 4(b). The reference values for the gaussian parameters are as in the following. *i) lateral simulation:* $\sigma_y = 0.0159s$, $A_y = 10^{-4}m$ for displacement and $A_\varphi$ for rotation; *ii) vertical simulation:* $\sigma_z = 0.0222s$, $A_z = 2\,10^{-2}m$ for displacement.

In Figure 5 the time-response functions obtained by the CFD simulation for lateral and vertical tank motion simulation are presented. In particular, Figs. 5(a) and 5(b) present the time histories of lateral force and moment on the tank as given by a lateral acceleration given by the input function in Fig. 4(b). Moreover, Figs. 5(c) and 5(d) present the time histories of lateral force and moment on the tank as given by a rotational acceleration, in turn, assigned by the input function in Fig. 4(b). Finally, in Fig. 5(d) the time history of the vertical force caused by a vertical acceleration as given by the input function in Fig. 4(b) is presented. It is worth pointing out that for all the sloshing CFD simulation cases presented, a linearity check was performed by considering the reference case for the Gaussian input function in Fig. 4 (Case 2), but also consider the same time input function but multiplied by $10^{-1}$ (Case 1), and finally the same input but multiplied by 2 (Case 3). All these case input were used for all the simulations in Fig. 5 but only the *lateral* simulations gave practically identical output when ever it divided by the associated amplification factor. This linearity check was not completely overcome by the vertical simulation (Fig. 5(e)) because of the presence of more relevant nonlinear phenomena,

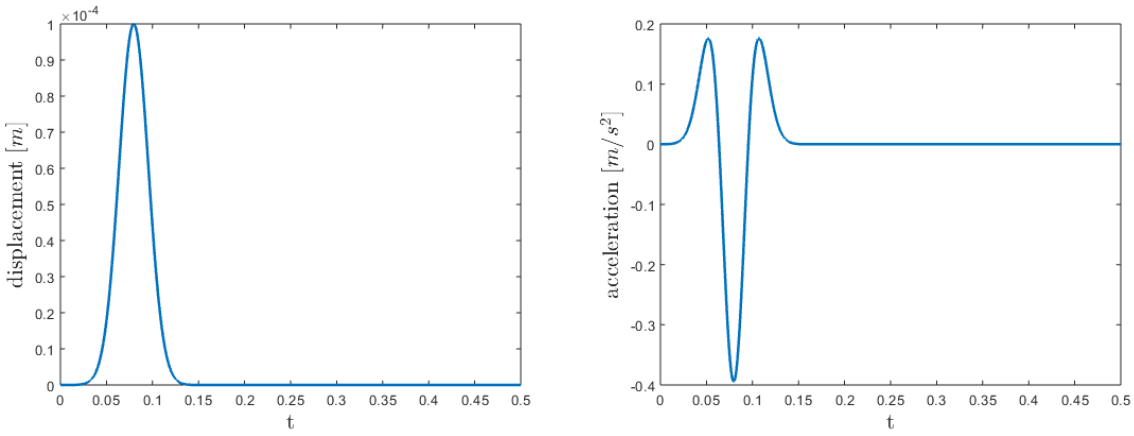


(a) Displacement trial function $q_t(t)$.

(b) Trial function second time derivative $\ddot{q}_t(t)$.

Figure 4: Trial input time function used as unsteady boundary conditions for the CFD code.

like Rayleigh–Taylor instabilities (that are present only in Case 2 and Case 3), also for small perturbations.

In Figure 6 and 7 the real and the imaginary parts of the lateral and vertical GSF matrices for the single considered tank (namely the matrix $\hat{\mathrm{G}}^{t_1}(\omega)$ and $\check{G}^{t_1}(\omega)$) are presented. In each figure a comparison between the directly CFD-obtained data and the interpolated data is presented.

The approximation reached for the all terms of the GSF transfer function matrix has so allowed to build the overall structure/tanks dynamical system representing the dynamic of the cantilever beam-like structure and the set of the seven sloshing tanks in Fig. 3 in the global form represented by the Eq. 18.

Figure 8 shows the scenario represented by the dynamical system poles in the complex plane in the case of frozen fluid (red markers) and sloshing fluid (blue markers) within the frequency bandwidth of interest of the problem from zero to 15 Hz so involving the first bending vibration mode of the cantilevered beam. More specifically, Fig. 8(a) presents the pole-system scenario without considering the vertical sloshing mechanism (*i.e.,* quantities with check symbol ˇ put equal to zero), whereas Fig. 8(b) presents the same scenario but including the vertical sloshing description, thus introducing an effect present at response conditions in which Rayleigh-Taylor instability occurs. It is apparent that the damping effect of the sloshing fluid arise mainly due to dissipation phenomena described by the vertical sloshing mechanism. The beam structural model includes a base modal damping of $\zeta_{beam} = -Re(s_1)/Im(s_1) = 0.01$ where $s_1$ is the red marked pole representing the first system damped mode without sloshing effects. By including the presented sloshing model this pole moves on left and gives a new value of the modal damping (blue marked) equal to $\zeta_{slo} = -Re(s_{1_{slo}})/Im(s_{1_{slo}}) = 0.0162$.

Finally, Figure 9 shows the results of the time response of the wing/fuel coupled system as given by an initial condition as in the experiment performed in Ref. [13] (indeed, an initial displacement field is imposed by applying a tip vertical load and subsequent release in the initial time, see model Eq. 6). As part of a wider project, a number of experiments have recently been performed at the Airbus Protospace Lab in Filton (Bristol, UK) to explore the effects of a tip tank containing a fluid on the motion of a beam subjected to moderate initial deflections and the subsequent release. The objective of this preliminary campaign was to

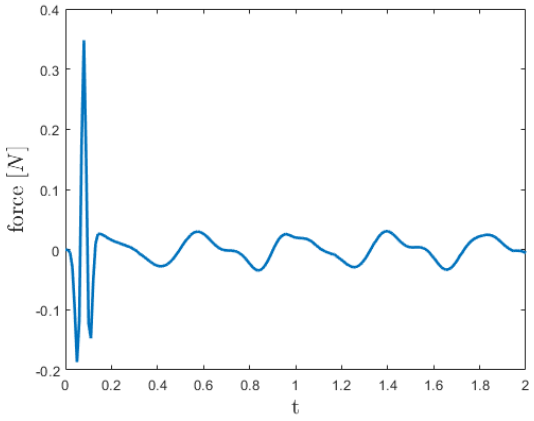


(a) Lateral force $f_y(t)$ as given by lateral displacement $y(t)$.

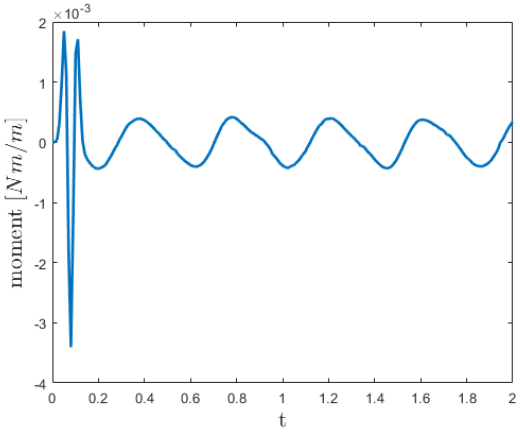


(b) Moment $M(t)$ as given by lateral displacement $y(t)$.

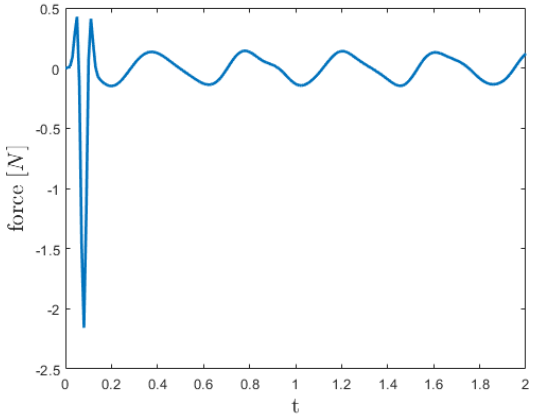


(c) Lateral force $f_y(t)$ as given by rotation $\varphi(t)$.

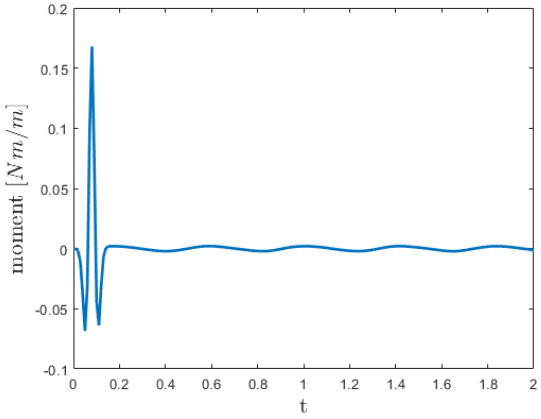


(d) Moment $M(t)$ as given by rotation $\varphi(t)$.

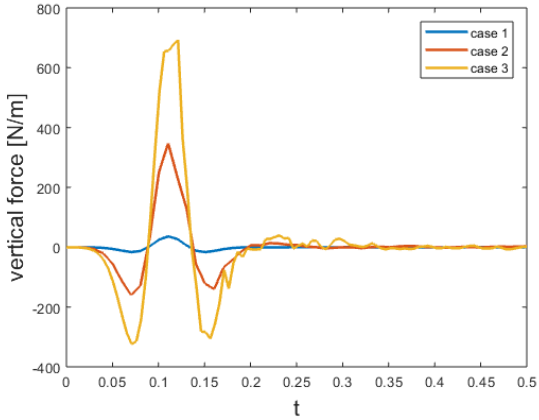


(e) Vertical force $f_z(t)$ as given by vertical displacement $z(t)$.

Figure 5: Output forces and moment evaluated by the CFD s imulation by the time acceleration input (displacements and rotations) given by the time function in Eq. 4(b).

prove that liquid sloshing affects significantly the damping characteristics of a free-vibrating wing-like structure, and therefore has the potential of alleviating dynamics loads if taken into

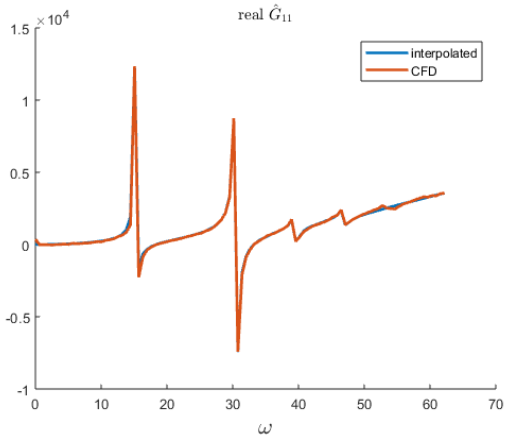


(a) Real parts of terms $\hat{G}_{CFD_{11}}(\omega)$ and $\hat{G}_{int_{11}}(\omega)$.

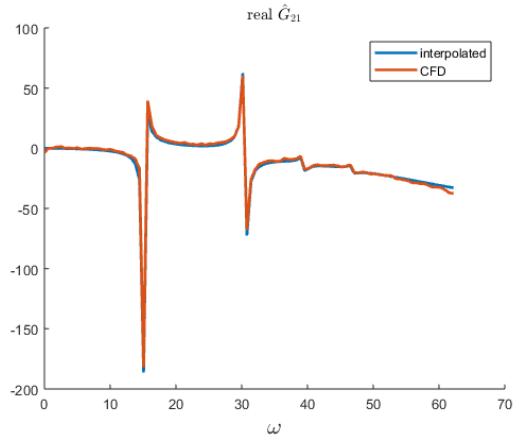


(b) Real parts of terms $\hat{G}_{CFD_{21}}(\omega)$ and $\hat{G}_{int_{21}}(\omega)$.

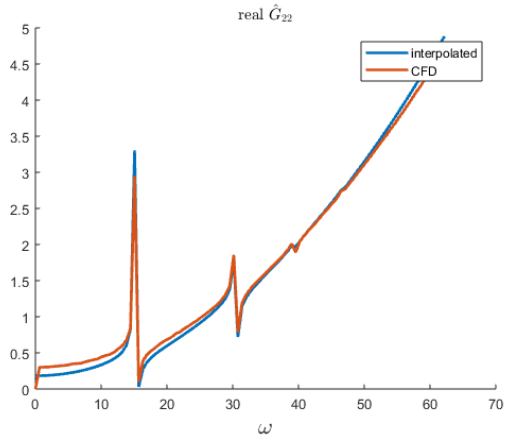


(c) Real parts of terms $\hat{G}_{CFD_{22}}(\omega)$ and $\hat{G}_{int_{22}}(\omega)$.

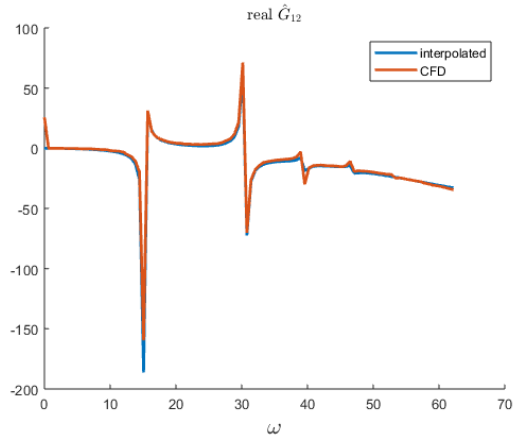


(d) Real parts of terms $\hat{G}_{CFD_{12}}(\omega)$ and $\hat{G}_{int_{12}}(\omega)$.

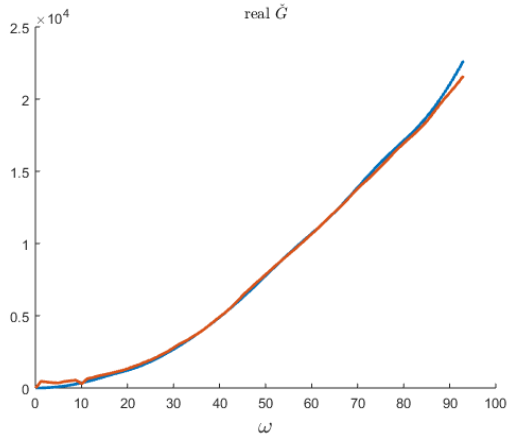


(e) Real parts of terms $\check{G}_{CFD}(\omega)$ and $\check{G}_{int}(\omega)$ for case 2.

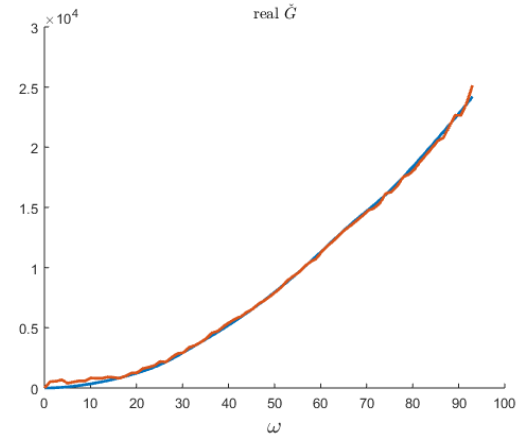


(f) Real parts of terms $\check{G}_{CFD}(\omega)$ and $\check{G}_{int}(\omega)$ for case 3.

Figure 6: Real parts of the entries of the $\hat{\mathsf{G}}_{CFD}(\omega)$ (lateral sloshing) and $\check{G}_{CFD}(\omega)$ (vertical sloshing) compared with the interpolating quantities $\hat{\mathsf{G}}_{int}(\omega)$ and $\check{G}(\omega)_{int}$.

account in the modelling. Figure 9 depicts the accelerometer vertical response at the beam tip (see Fig. 3) as given by the measurement and that obtained by the presented cfd-based ROM model in the case of frozen and sloshing fluid. In Figure 9 the experimental acceleration time

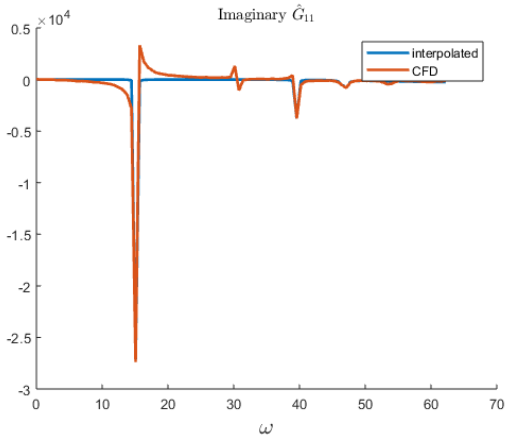


(a) Imaginary parts of terms $\hat{G}_{CFD_{11}}(\omega)$ and $\hat{G}_{int_{11}}(\omega)$.

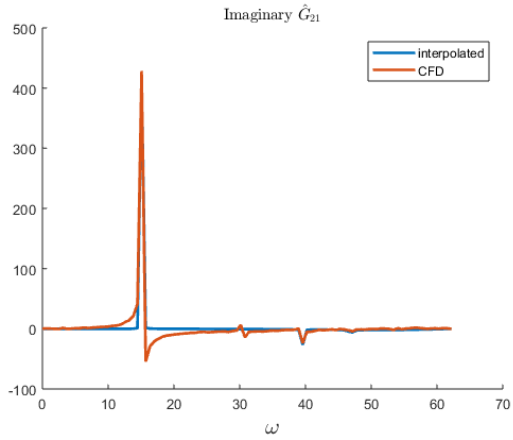


(b) Imaginary parts of terms $\hat{G}_{CFD_{21}}(\omega)$ and $\hat{G}_{int_{21}}(\omega)$.

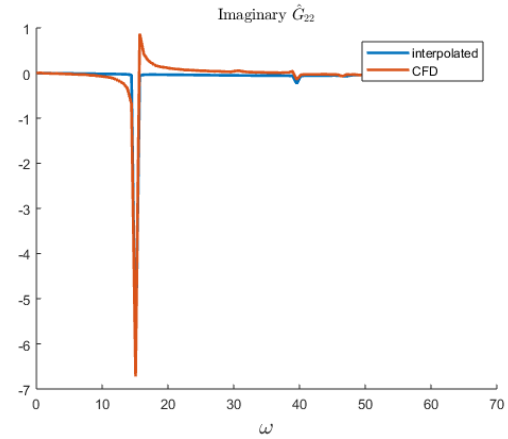


(c) Imaginary parts of terms $\hat{G}_{CFD_{22}}(\omega)$ and $\hat{G}_{int_{22}}(\omega)$.

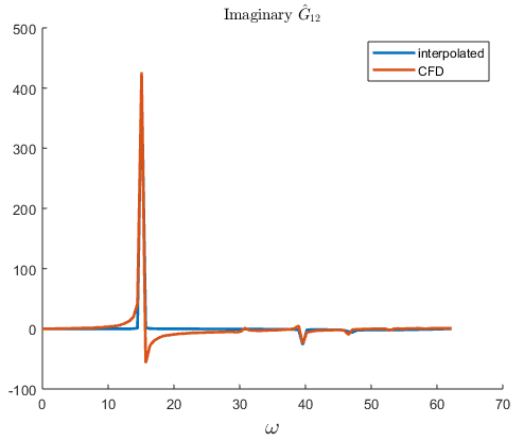


(d) Imaginary parts of terms $\hat{G}_{CFD_{12}}(\omega)$ and $\hat{G}_{int_{12}}(\omega)$.

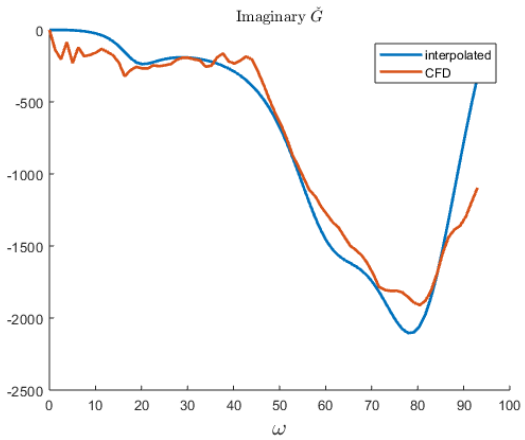


(e) Imaginary parts of terms $\check{G}_{CFD}(\omega)$ and $\check{G}_{int}(\omega)$ for case 2.

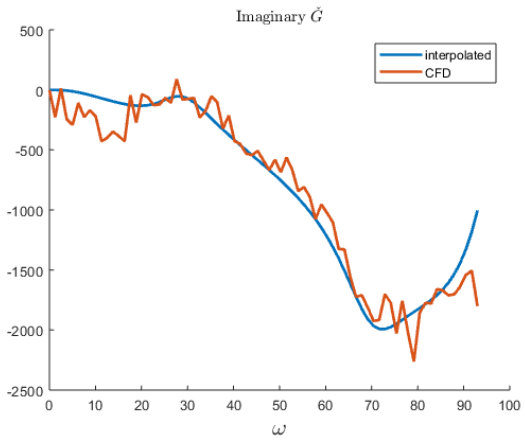


(f) Imaginary parts of terms $\check{G}_{CFD}(\omega)$ and $\check{G}_{int}(\omega)$ for case 3.

Figure 7: Imaginary parts of the entries of the $\hat{\mathsf{G}}_{CFD}(\omega)$ (lateral sloshing) and $\check{G}_{CFD}(\omega)$ (vertical sloshing) compared with the interpolating quantities $\hat{\mathsf{G}}_{int}(\omega)$ and $\check{G}(\omega)_{int}$.

history (purple curve) is compared with the numerical result given by the frozen model (blue curve), the result including only the lateral slosh modelling (red dashed curve), and the result

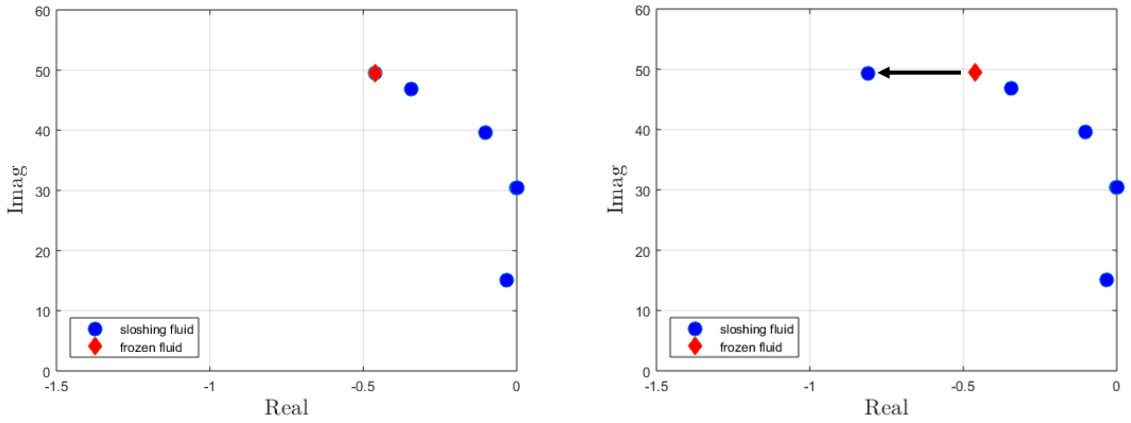


(a) Vertical sloshing off. (b) Vertical sloshing on.

Figure 8: Poles of the coupled wing-structures/fuel-sloshing system. Blue markers represent the poles of the coupled system, red markers the poles of frozen fluid system.

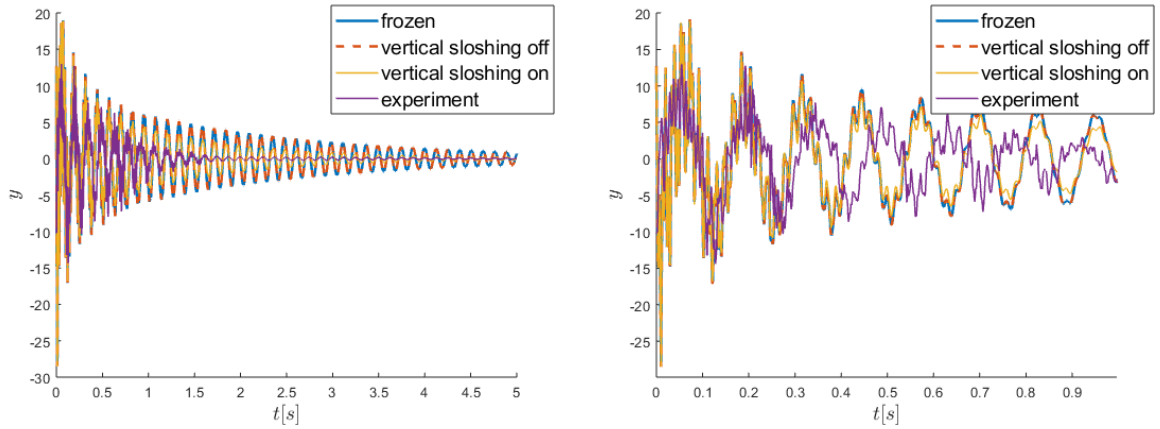


(a) first 5 seconds. (b) zoom on first second.

Figure 9: Free responses simulating the experiment conditions in Ref. [13] and here simulated in the case of frozen fuel and sloshing fuel by the introduced CFD-based model.

icluding the model improved by the vertical sloshing model (yellow curve). If one considers the zoom of the picture in the first second (Fig. 9(b)), one can notice that the experimental data presents a nonlinear behaviour consisting of a frequency/damping content variating in time. This nonlinear signature has been widely studied in Ref. [14] and it cannot be represented by the here proposed linearized CFD-based ROM. However, the capability of the ROM model to perform the coupled oscillation is apparent although the estimated damping level is lower and frequency shift behavior not represented.

## 5 CONCLUDING REMARKS

In the present paper a Reduced-Order Models (ROM) based on data provided by a high-fidelity and highly efficient CFD code, for the study of sloshing-integrated aeroelastic systems is proposed. A sloshing-addressed CFD code, ELEMENTAL®, is employed to generate data set to be used for the ROM synthesis.

The developed sloshing ROM, based on a Linearized Frequency Domain (LFD) approach, uses an Input/Output system identification technique from CFD transient simulations to construct an

unsteady Generalized Sloshing Force (GSF) matrix in analogy with the Generalized Aerodynamic Force (GAF) matrix used to model the aircraft external unsteady aerodynamics. Furthermore, a frequency-domain interpolation technique applied on the obtained GSF matrix allowed to represent the overall structure/fluid-sloshing system as an Equivalent Mechanical Model system in modal co-ordinate.

Sloshing ROM has been modelled by distinguishing *lateral* and *vertical* sloshing motion. The lateral sloshing proposed model (LFD and finite-state interpolation) within the basic hypothesis of small perturbations, may be generalized in terms of tank geometry and rigid body motion: in the presented case study this behavior revelaed not so relevant on influency the overall wing dynamics. The vertical sloshing behavior is the most critical for the influence on the global dynamics but it is also the most characterised by nonlinear effects and, therefore, the effectiveness of the linearized approach resulted to be weaker for it. Therefore, GSF identification procedure using different levels of exication for the sloshing CFD should be explored in future for better representing this phenomenon by ROM.

The obtained results will allow to apply this approach for future fast aeroelastic analyses to be performed in the design phase. The results concerning the unsteady effects induced by sloshing interacting with the wing structure is first compared directly with experimental data for evaluating the effectiveness of applicability of such a state-space fast representation for perspective aeroelastic analyses and design.

## 6 REFERENCES

[1] Farhat, C., Amsallem, D., "Recent Advances in Reduced-Order Modeling and Application to Nonlinear Computational Aeroelasticity," 46th AIAA Aerospace Sciences Meeting and Exhibit Reno, Nevada, AIAA 2008-562, 2008.

[2] Sykes, B.S., Malan, A., G., Gambioli, F., "Novel Nonlinear Fuel Slosh Surrogate Reduced-Order Model for Aircraft Loads Prediction," *AIAA - Journal of Aircraft,* Vol. 55, No. 3, May-June, 2018, pp. 1004-1013.

[3] Oxtoby, O.F., Malan, A., G., Heyns, J. A., "A computationally efficient 3D finite-volume scheme for violent liquid–gas sloshing," *International Journal for Numerical Methods in Fluids,* Vol. 79, 2015, pp. 306-321.

[4] Capri, F., Mastroddi, F., Pizzicaroli, A., "A Linearized Aeroelastic Analysis for a Launch Vehicle in Transonic Flow," *AIAA - Journal of Spacecraft and Rockets,* Vol. 43, No. 1, Jan-Feb 2006, pp. 92-104.

[5] Mastroddi, F., Stella, F., Cantiani, D., Vetrano, F., "Linearized Aeroelastic Gust Response Analysis of a Launch Vehicle ", *AIAA - Journal of Spacecraft and Rockets*, Vol. 48, No. 3, May-June 2011, pp. 196-206.

[6] Castronovo, P., Mastroddi, F., Stella, F., Biancolini, M.E., "Assessment and Development of a ROM for Linearized Aeroelastic Analyses of Aerospace Vehicles ", *CEAS Aeronautical Journal*, Vol. 8, N. 2, June 2017, pp. 353-369.

[7] Gambioli, F., Malan, A., "Fuel Loads in Large Civile Airplanes," International Forum on Aeroelasticity and Structural Dynamics, IFASD 2017 25-28 June 2017, Como, Italy, paper n. 238.

[8] Karpel, M., "Design for the Active Flutter Suppression and Gust Alleviation Using State-Space Aeroelastic Modeling," *Journal of Aircraft,* Vol. 19, No. 3, 1982, pp. 221-227.

[9] Morino, L., Mastroddi, F., De Troia, R., Ghiringhelli, G.L., Mantegazza, P., "Matrix Fraction Approach for Finite-State Aerodynamic Modeling," *AIAA Journal,* Vol. 33. No. 4, April 1995, pp. 703-711.

[10] Gennaretti, M., Mastroddi, F., "Study of Reduced-Order Models for Gust-Response Analysis of Flexible Wings," *Journal of Aircraft,* Vol. 41, No.2, March-April 2004, pp. 304-313.

[11] Abramson, H., N., "The Dynamic Behavior of Liquids in Moving Containers, with Applications to Space Vehicle Technology," NASA-SP-106, 1966.

[12] Ibrahim, R., *Liquid Sloshing Dynamics: Theory and Applications,* Cambridge: Cambridge University Press, 2005

[13] Gambioli, F., Alegre Usach, R., Kirby, J., and Wilson, T., "Experimental Evaluation of Fuel Sloshing Effects on Wing Dynamics," *International Forum on Aeroelasticity and Structural Dynamics,* IFASD 2019, Savannah, GE, 9-13 June 2019.

[14] Titurus, B., Cooper, J.E., Saltari, F., Mastroddi, F., Gambioli, F., "Analysis of a sloshing beam experiment," *International Forum on Aeroelasticity and Structural Dynamics,* IFASD 2019, Savannah, GE, 9-13 June 2019.

## COPYRIGHT STATEMENT